

# Communications with Guaranteed Low Latency and Bandwidth using Frequency Referenced Multiplexing

Zichuan Zhou<sup>1</sup>, Jinlong Wei<sup>2</sup>✉, Yuan Luo<sup>3</sup>✉, Kari A. Clark<sup>1</sup>, Eric Sillekens<sup>1</sup>,  
Callum Deakin<sup>1</sup>, Ronit Sohanpal<sup>1</sup>, Radan Slavík<sup>4</sup>, and Zhixin Liu<sup>1</sup>✉

<sup>1</sup>Optical Networks Group, University College London, London, UK

<sup>2</sup>Huawei Technologies Duesseldorf GmbH, European Research Centre, Munich, Germany

<sup>3</sup>The Chinese University of Hong Kong (Shenzhen), Shenzhen, China

<sup>4</sup>Optoelectronic Research Centre, University of Southampton, Southampton, UK

## I BER and sensitivity characterisation

The receiver power sensitivities shown in figure 4 were calculated based on the bit error ratio (BER) measurement for each live user. Here we show the example BER measurement of the live user upstream signals using subcarrier modulation (SCM) with 4/8/16 QAM formats.

The BER is measured by varying the optical power into EDFA 3 using a variable optical attenuator (VOA), as shown in figure 3a. The power per user channel was measured using an optical spectrum analyser (OSA) of 0.01nm resolution. The each BER value is calculated using a pseudorandom binary sequence (PRBS) of  $2^{15}$  length and one-by-one comparison between recovered bits and transmitted bits. Example BER curves are shown in figure S1 for all three live users channels with user 1 locating at the centre of the spectrum and user 2 and 3 locked to 2.5 GHz spacing apart (see figure 4b). Two examples are shown here to illustrate the BER performance and the calculation of receiver power sensitivities. They are locked to neighboring channels at the center (channel 1-3, 193.412 – 193.417 THz, closed markers as indicated in figure S1a-c) and the edge (channel 29-31, 193.482 – 193.487 THz, open markers as indicated in figure S1d-f) of the optical bandwidth, respectively. Their frequency offset to center wavelength (i.e., the LO wavelength) is  $\Delta f = i \times 2.5\text{GHz}$ , where  $i$  is the channel ID. User 1 exhibited about 4 dB higher sensitivity than user 2 and user 3 irrespective of modulation format. This performance difference is mainly due to the EAMs used in the user transceivers. The EAM in user 1 is optimised for 1550 nm, while the EAMs for user 2 and user 3 are optimised for 1535 nm. Compared to center channels, edge channels exhibit worse BER performance due to the frequency roll-off of coherent receiver. Considering user 1 with 2.5 GHz offset from the LO, the sensitivities for the SCM formats of 4, 8 and 16 QAM at the hard-decision forward error correction (HD-FEC) threshold of  $4.4\text{e-}3$  (6.7% overhead) were -44, -35 and -29 dBm, respectively. The sensitivities at the soft-decision (SD) threshold of  $2\text{e-}2$  (15.3% overhead) were -47, -40 and -35 dBm, respectively, for the SCM with formats of 4/8/16QAM.

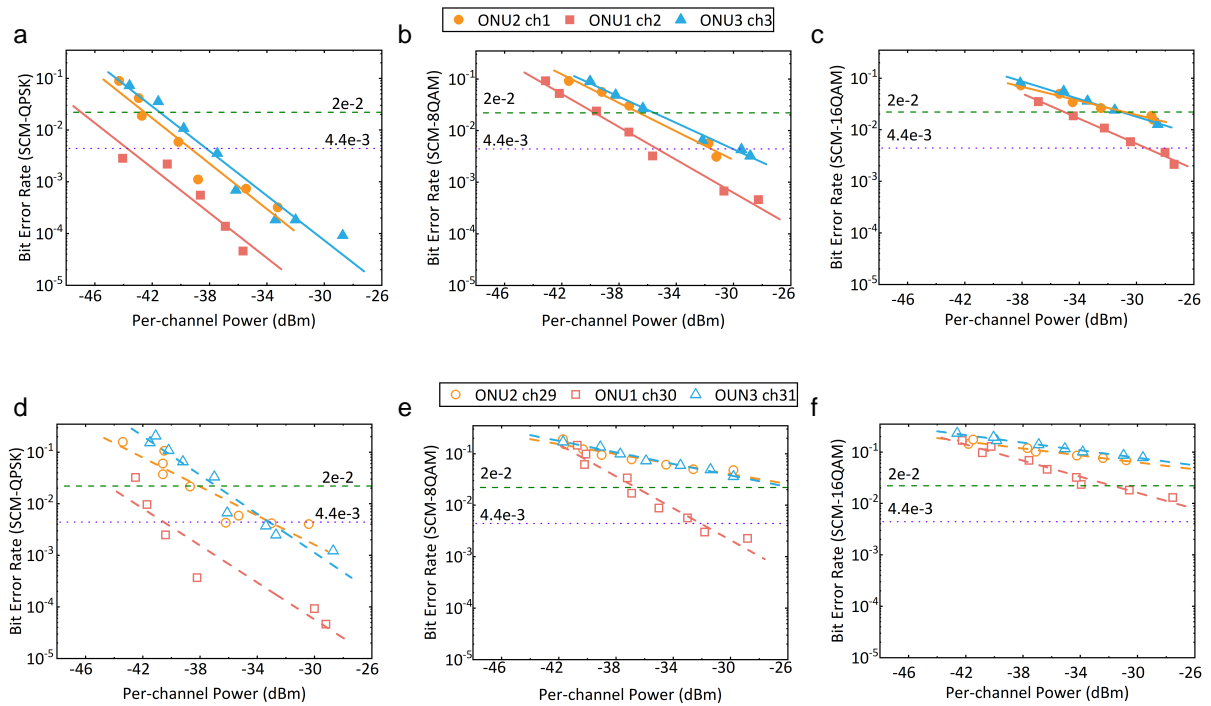


Fig. S 1: BER sensitivities of the ONUs locked at the receiver spectrum center (solid markers, channel 1-3) using SCM formats (a) 4 QAM; (b) 8 QAM; (c) 16 QAM and locked at receiver spectrum edge (open markers, channel 29-31) using SCM formats (d) 4 QAM; (e) 8 QAM; (f) 16 QAM

## II SD-FEC receiver sensitivity of user 2 and 3 over 160 GHz

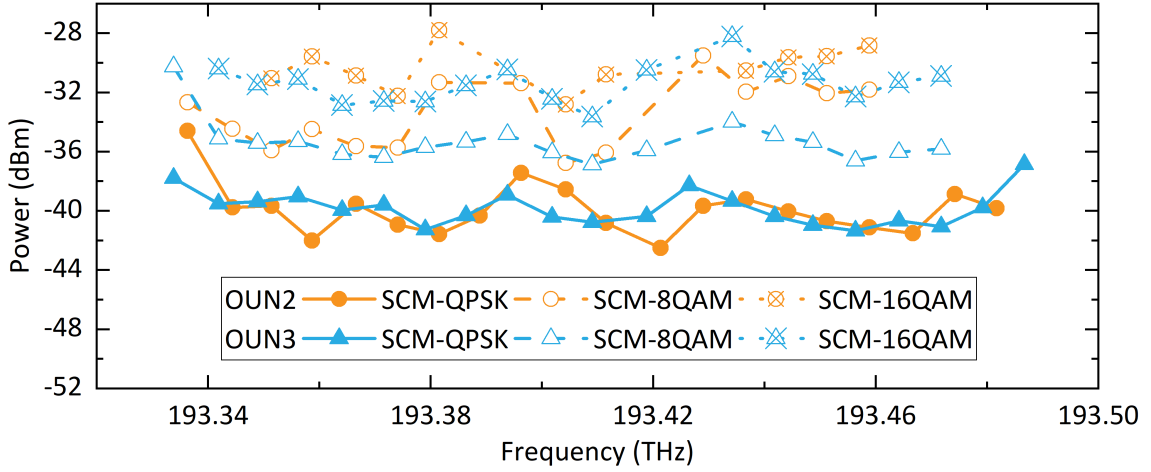


Fig. S 2: Upstream receiver sensitivity at SD-FEC threshold BER of  $2e-2$  for user 2 and user 3.

Similar to the results shown in figure 4d, we characterise receiver sensitivities for user 2 and user 3 by measuring the BER vs per-user power across the whole 160 GHz bandwidth. This was achieved by tuning the lasers at both user 2 and user 3 (together with user 1) from -80 GHz to 80 GHz frequency offset. Compared to user 1 signal demonstrated in the paper (figure 4d), the sensitivities of user 2 and user 3 are approximately 4 dB lower due to the EAM used, which has lower extinction ratio at 1550 nm than the user 1 EAM. This performance difference could be avoided by using low-loss wavelength insensitive modulator such as thin-film  $LiNbO_3$  modulators [1, 2].

### III Dynamic Range characterisation

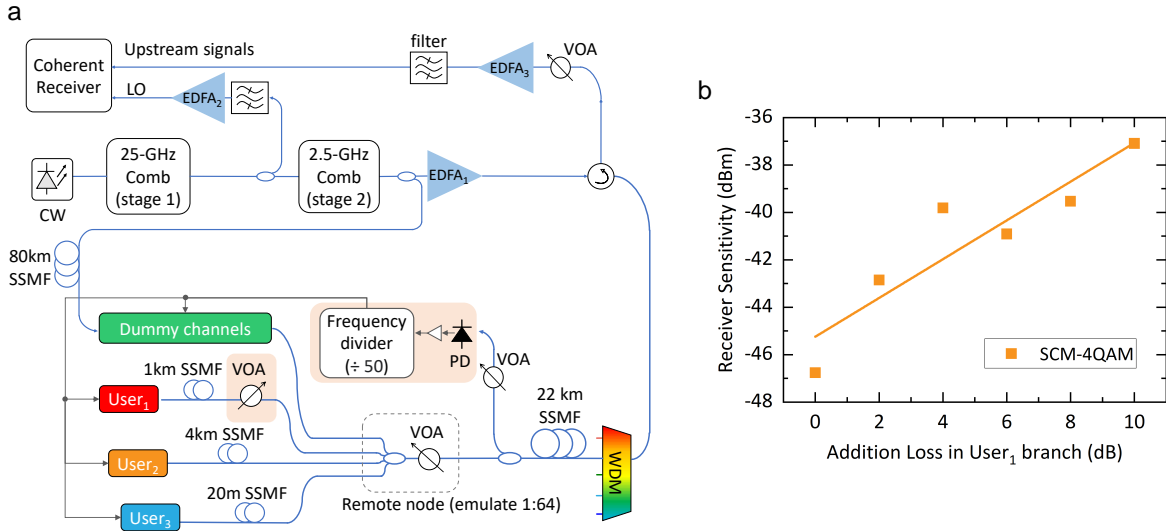


Fig. S 3: (a) Experimental setup for dynamic range characterization; (b) Dynamic range characterization using SCM-4QAM.

In practice, optical power from different users may vary due to the different fibre lengths and splitting loss. Here we characterise the tolerance to user signal power variation by introducing a VOA in the user 1 branch, as shown in figure S3. Similar to the experiments shown in figure 4a-c, the wavelength of user 1 is aligned to the centre of the WDM band (channel #1) and user 2 and 3 are aligned to the neighbouring FDM channels. By introducing additional loss using the VOA in the user 1 branch, we measure the receiver power sensitivities at the BER of  $2e-2$  for the user 1 upstream signals of SCM-4QAM modulation. With 10 dB additional attenuation, the receiver sensitivity is degraded from -47 dBm to -37 dBm. The results indicate that the signal is ASE noise limited due to the EDFA before the coherent receiver.

## IV Transmitter and Receiver DSP chain

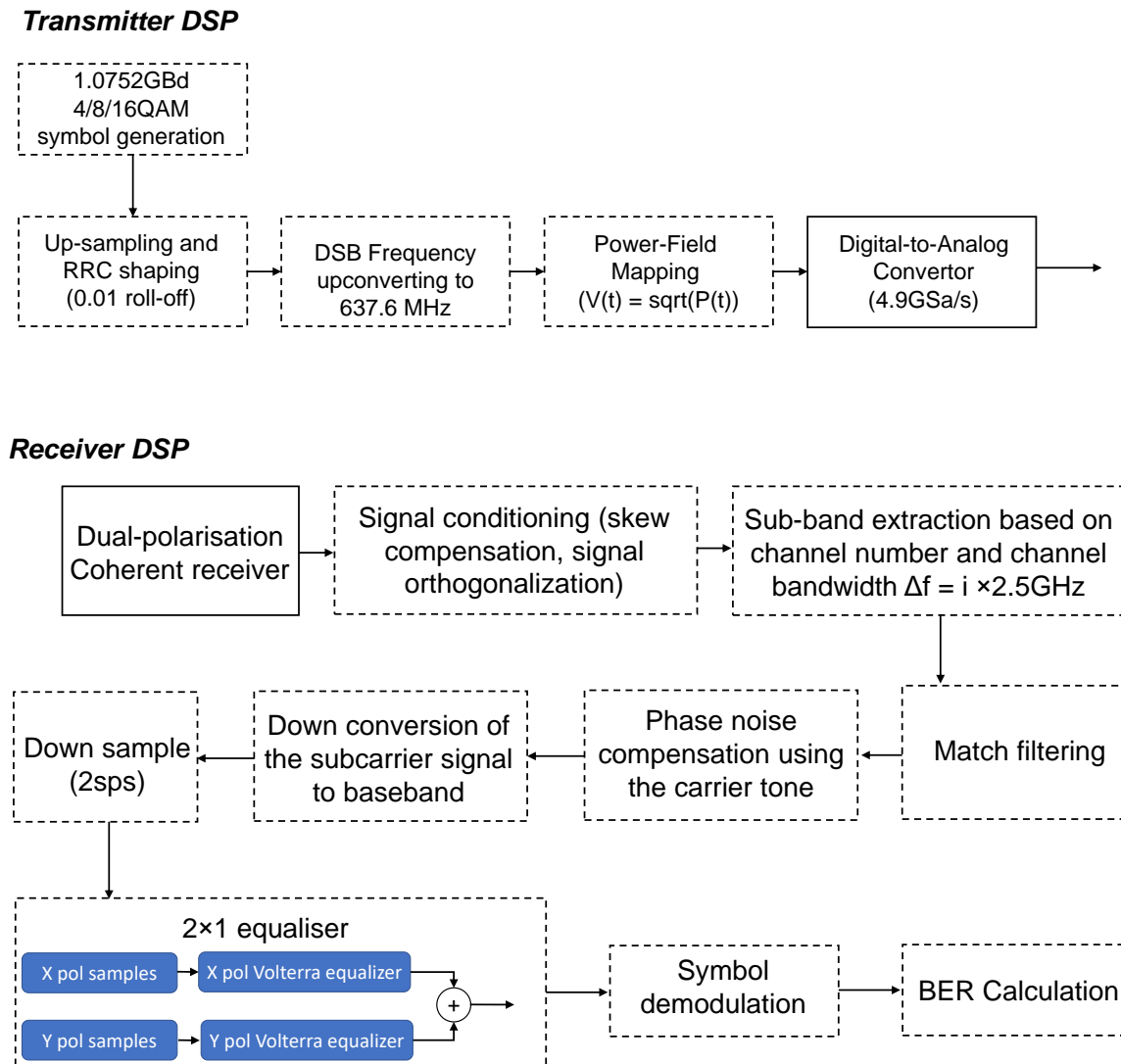


Fig. S 4: Transmitter and Receiver DSP chain.

## References

- [1] Wang, C. *et al.* Integrated lithium niobate electro-optic modulators operating at CMOS-compatible voltages. *Nature* **562**, 101–104 (2018).
- [2] He, M. *et al.* High-performance hybrid silicon and lithium niobate Mach–Zehnder modulators for 100 Gbps and beyond. *Nature Photonics* **13**, 359–364 (2019).